

Original Article



L-arginine promotes angio-osteogenesis to enhance oxidative stress-inhibited bone formation by ameliorating mitophagy

Yang Shen^{a,b,1}, Haoming Wang^{a,b,1}, Hongwei Xie^{a,b,1}, Jiateng Zhang^{a,b}, Qingliang Ma^{a,b},
Shiyu Wang^{a,b}, Putao Yuan^{a,b}, Hong Xue^{a,b}, Huaxing Hong^c, Shunwu Fan^{a,b,***},
Wenbin Xu^{a,b,**}, Ziang Xie^{a,b,*}

^a Department of Orthopaedic Surgery, Sir Run Run Shaw Hospital, Zhejiang University School of Medicine, Hangzhou, China

^b Key Laboratory of Musculoskeletal System Degeneration and Regeneration Translational Research of Zhejiang Province, Hangzhou, China

^c Department of Orthopaedics, Taizhou Hospital of Zhejiang Province, Wenzhou Medical University, Taizhou, China

ARTICLE INFO

Keywords:
angiogenesis
L-arginine
mitophagy
Osteogenesis

ABSTRACT

Background: Osteoporosis is one of the most common bone diseases in middle-aged and elderly populations worldwide. The development of new drugs to treat the disease is a key focus of research. Current treatments for osteoporosis are mainly directed at promoting osteoblasts and inhibiting osteoclasts. However, there is currently no ideal approach for osteoporosis treatment. L-arginine is a semi-essential amino acid involved in a number of cellular processes, including nitric production, protein biosynthesis, and immune responses. We previously reported that L-arginine-derived compounds can play a regulatory role in bone homeostasis.

Purpose: To investigate the specific effect of L-arginine on bone homeostasis.

Methods: Mildly aged and ovariectomized mouse models were used to study the effects of L-arginine on osteogenesis and angiogenesis, assessed by micro-computed tomography and immunostaining of bone tissue. The effect of L-arginine on osteogenesis, angiogenesis, and adipogenesis was further studied in vitro using osteoblasts obtained from cranial cap bone, endothelial cells, and an adipogenic cell line. Specific methods to assess these processes included lipid staining, cell migration, tube-forming, and wound-healing assays. Protein and mRNA expression was determined for select biomarkers.

Results: We found that L-arginine attenuated bone loss and promoted osteogenesis and angiogenesis. L-arginine increased the activity of vascular endothelial cells, whereas it inhibited adipogenesis in vitro. In addition, we found that L-arginine altered the expression of PINK1/Parkin and Bnip3 in the mitochondria of osteoblast-lineage and endothelial cells, thereby promoting mitophagy and protecting cells from ROS. Similarly, L-arginine treatment effectively ameliorated osteoporosis in an ovariectomized mouse model.

Conclusion: L-arginine promotes angio-osteogenesis, and inhibits adipogenesis, effects mediated by the PINK1/Parkin- and Bnip3-mediated mitophagy.

The Translational Potential of this Article: L-arginine supplementation may be an effective adjunct therapy in the treatment of osteoporosis.

1. Introduction

Bone remodeling is critical for bone homeostasis. Once skeletal cells are inhibited or abnormally active, this balance is disrupted, leading to osteoporosis [1]. The incidence of osteoporosis, an age-related systemic

skeletal disorder, has remained high among the elderly population in recent years. One in three women and one in five men are at risk of bone fractures caused by osteoporosis [2]. This increased bone fragility and susceptibility to fractures greatly reduce the quality of life of these patients [3,4]. Antiresorptive therapies currently available for

* Corresponding author. Department of Orthopaedic Surgery, Sir Run Run Shaw Hospital, Zhejiang University School of Medicine, Hangzhou, China.

** Corresponding author. Department of Orthopaedic Surgery, Sir Run Run Shaw Hospital, Zhejiang University School of Medicine, Hangzhou, China.

*** Corresponding author. Department of Orthopaedic Surgery, Sir Run Run Shaw Hospital, Zhejiang University School of Medicine, Hangzhou, China.

E-mail addresses: 0099203@zju.edu.cn (S. Fan), xuwenbin@zju.edu.cn (W. Xu), ziang_xie@zju.edu.cn (Z. Xie).

¹ These authors contributed equally to this work.

osteoporosis, including denosumab and bisphosphonates, and anabolic medications, such as parathyroid hormone, have been used clinically to reduce bone resorption or stimulate bone formation. However, in addition to their therapeutic effects, these drugs have side effects that cannot be ignored. Therefore, natural biological agents that can promote angio-osteogenesis and attenuate osteoclastogenesis with fewer side effects are required to treat osteoporosis [5,6].

Autophagy refers to the process through which parts of the cell are degraded in the lysosome; it plays an irreplaceable role in the homeostasis of cells, tissues, and organs. Many autophagy-related genes have clear etiological correlations with human diseases [7,8]. Autophagy not only maintains intracellular nutrition through the degradation of intracellular components but also selectively eliminates organelles to maintain the organellar balance in terms of quantity and quality. Bone homeostasis is also closely related to autophagy, which can modulate this process by affecting osteoblasts, osteoclasts, osteocytes, and other bone tissues [9]. Mitophagy is a specific type of autophagy that targets damaged mitochondria [10]. When mitochondria are damaged, continuous depolarization occurs in the inner membrane, which stabilizes phosphatase and tensin homolog deleted on chromosome ten (PTEN)-induced kinase 1 (PINK1), resulting in the recruitment of Parkin to the outer mitochondrial membrane. Parkin ubiquitinates proteins and recruits mitochondria to the autophagic pathway [11,12]. The PINK1/Parkin-related pathway is the primary mitophagic pathway, especially in Parkinson's disease. Several studies have demonstrated that BCL2 and adenovirus E1B 19 kDa-interacting protein3 (Bnip3) play a significant role in mitophagy [13,14]. Moreover, recent studies have shown that mitochondrial reactive oxygen species (ROS) level is limited by Bnip3-associated mitochondrial autophagy and that a relationship exists between mitochondrial ROS production and Bnip3 expression [15].

L-arginine participates in various key physiological and biochemical activities in the human body. It is a component of the body's defense against pathogen invasion and is used as a dietary supplement to promote muscle strength recovery [16,17]. L-arginine is a key substrate for the synthesis of NO and can be converted to urea and L-ornithine through the action of arginase. In adults, L-arginine is used to produce citrulline and ornithine in quantities sufficient to meet the requirements of the urea cycle. However, L-arginine may become conditionally essential in some situations and, therefore, must be provided in the diet. For example, in neonates and children, the amount of L-arginine produced in the body during development is insufficient for growth, whereas, in the elderly population, endogenous L-arginine synthesis is lacking. Previous studies have shown that L-arginine supplementation promotes thymic regrowth and reactivation of thymic function in aged animals [18]. In addition, we previously found that mechanical force can regulate asymmetric dimethylarginine dimethylamine hydrolase 1 in osteoblasts [19], suggesting that L-arginine-derived compounds might play a regulatory role in bone homeostasis. However, the association between mitophagy and L-arginine has not been fully elucidated in previous bone-remodeling studies. Accordingly, the aim of our study was to investigate whether L-arginine can alleviate osteoporosis, explore whether it can alter cell differentiation through its effect on mitochondria, and determine whether it can be used as an adjunct supplement therapy in the treatment of osteoporosis.

2. Methods

2.1. Chemicals and reagents

L-arginine was obtained from Solarbio (A0013, Beijing, China). S-(2-Boronethyl)-L-Cysteine hydrochloride (BEC-HCl) was obtained from Selleck (Shanghai, China, S7929). Fetal bovine serum (FBS) and Dulbecco's modified Eagle's medium (DMEM) were purchased from Gibco (Carlsbad, USA). The minimal essential medium (MEM) was from

Procell (Wuhan, China). Antibodies against BNIP3 and Runt-related transcription factor 2 (RUNX2) were purchased from Abcam (Cambridge, USA). Antibodies against PINK1, Parkin, peroxisome proliferator-activated receptors γ (PPAR γ), fatty acid binding protein 4 (FABP4), and CCAAT/enhancer binding protein γ (CEBP γ) were purchased from Proteintech (Wuhan, China). Cell Counting Kit-8 was purchased from Dojindo Molecular Technology (Kumamoto, Japan).

2.2. Osteogenic differentiation assay

Osteoblasts were isolated from the cranial cap bone of C57BL/6 mice (3 d postnatal), as previously reported [20]. Osteoblasts were seeded in 24-well plates with DMEM-based osteogenic induction medium (10% FBS, 50 mM L-ascorbic acid 2-phosphate, and 10 mM β -glycerophosphate) and cultured in a conditioned incubator. Osteoblasts were stained with alkaline phosphatase (ALP; CWBio, Beijing) and alizarin red solution (ARS; Cyagen Biosciences, Guangzhou, China) at 7 d and 21 d, respectively.

2.3. Adipogenic differentiation assay

C3H10 cells were seeded in 24-well plates with MEM-based adipogenic induction medium (10% FBS, 0.5 mM isobutylmethylxanthine, 0.25 μ M dexamethasone, and 1 μ g/mL insulin) and cultured in a conditioned incubator. The degree of adipogenic differentiation of cells was assessed using an Oil red O staining kit (Jiancheng, Nanjing, China).

2.4. Cell migration and invasion assays

Cell invasion assays were performed in 24-well transwell chambers (Corning, Tewksbury, USA). Human umbilical vein endothelial cells (HUVECs) were seeded inside transwell inserts with 200 μ L of specific medium. Then, 600 μ L of the medium was placed into the lower chamber. HUVECs located at the lower surface of the filters were fixed, stained with 0.1% crystal violet solution, and counted under a light microscope.

2.5. Tube forming assay

After the specific treatment protocol, HUVECs were seeded in 96-well plates with Matrigel (Corning) and incubated in a conditioned incubator. Cells were observed continuously for 2 h under a light microscope.

2.6. Wound-healing assay

HUVECs were seeded in six-well plates and scratched with a 200 μ L pipette tip when the cell density reached approximately 80%. Images of the wounds were captured from the same vantage point at 0 and 12 h post-injury. ImageJ software (National Institutes of Health; Bethesda, USA) was used to quantify the ratio of the initial wound area to the wound area remaining at 12 h.

2.7. RNA extraction assay

Total RNA was extracted using the Ultrapure RNA Kit (CWBio). Complementary DNA (cDNA) was synthesized from the RNA with a 10 μ L system containing RNase-free water, 5 \times PrimeScript RT Master Mix (Takara Bio, Otsu, Japan). Then, cDNA was mixed with SYBR Green Master Mix (Yeason, Beijing, China), and RT-PCR experiments were performed using an ABI Prism 7500 system (Applied Biosystems, USA). The reaction parameters were stated as previously reported [21]. Primer sequences used for real-time RT-PCR are shown in Table S1. β -Actin expression was used to normalize the expression of target genes. Results were analyzed using the $\Delta\Delta$ Ct method.

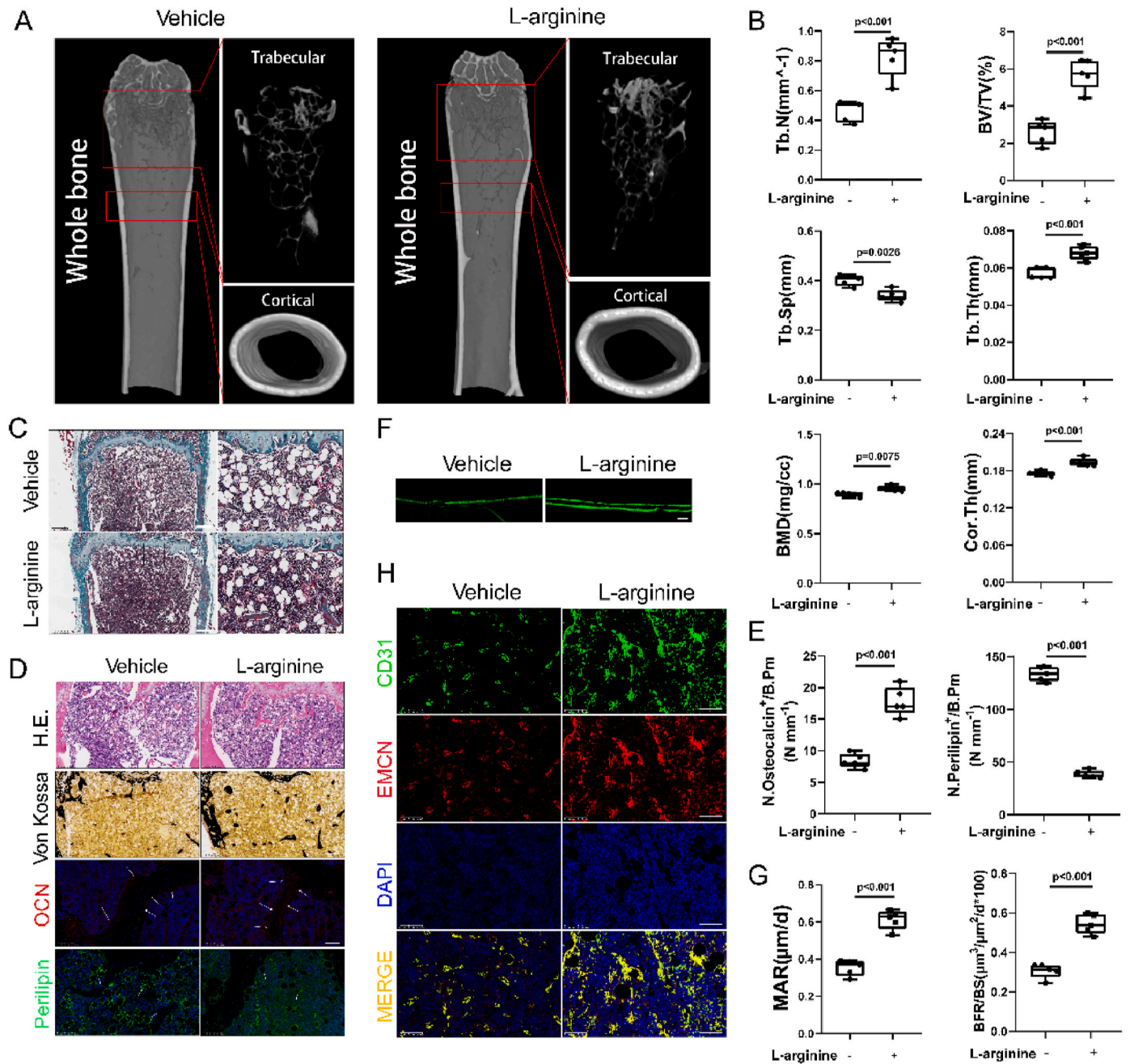


Figure 1. L-arginine promotes bone formation in aged mice. (A) Representative micro-CT images of proximal femurs from vehicle group and L-arginine group. (B) Quantitative analyses of BV/TV, Tb.N, Tb.Sp, Tb.Th, Cor.Th and BMD (n = 5 per group). (C) Representative images of Masson staining of decalcified bone sections from 2 groups. Scale bar = 300 μm . (D) Representative images of H.E., Von Kossa, OCN and perilipin staining of femurs from 2 groups. Scale bar = 200 μm . (E) Quantitative analyses of OCN and Perilipin positive cells in femora (n = 5 per group). (F) Representative images of Calcein double fluorescent labeling in mouse femurs. Scale bar = 5 μm . (G) Quantitative analyses of MAR and BFR/BS (n = 5 per group). (H) Immunostaining of CD31 (green) and EMCN (red) in femurs. Scale bar = 50 μm . (For interpretation of the references to color in this figure legend, the reader is referred to the Web version of this article.)

2.8. Western blot analysis

After cell treatments, the cells were lysed with RIPA lysis buffer, and total protein was extracted. Proteins were separated via SDS-PAGE using 8% or 10% gels and transferred onto polyvinylidene fluoride membranes. Membranes were blocked in 5% FBS buffer for 60 min at room temperature and then incubated overnight with specific primary antibodies at 4 °C. The next day, membranes were incubated with secondary antibodies for 60 min at room temperature. Target bands were visualized using a LAS-4000 Science Imaging System (Fujifilm, Tokyo, Japan).

2.9. Flow cytometry

HUVECs, osteoblasts, and C3H10 cells were seeded in six-well plates and treated as required. Mitochondrial membrane potential was evaluated using a JC-1 kit (C2003S; Beyotime, Shanghai, China). Samples were analyzed using an Accuri C6 flow cytometer (BD Biosciences, San Diego, USA).

2.10. Immunofluorescence staining

Cells were fixed and permeabilized with 0.5% Triton X-100. After

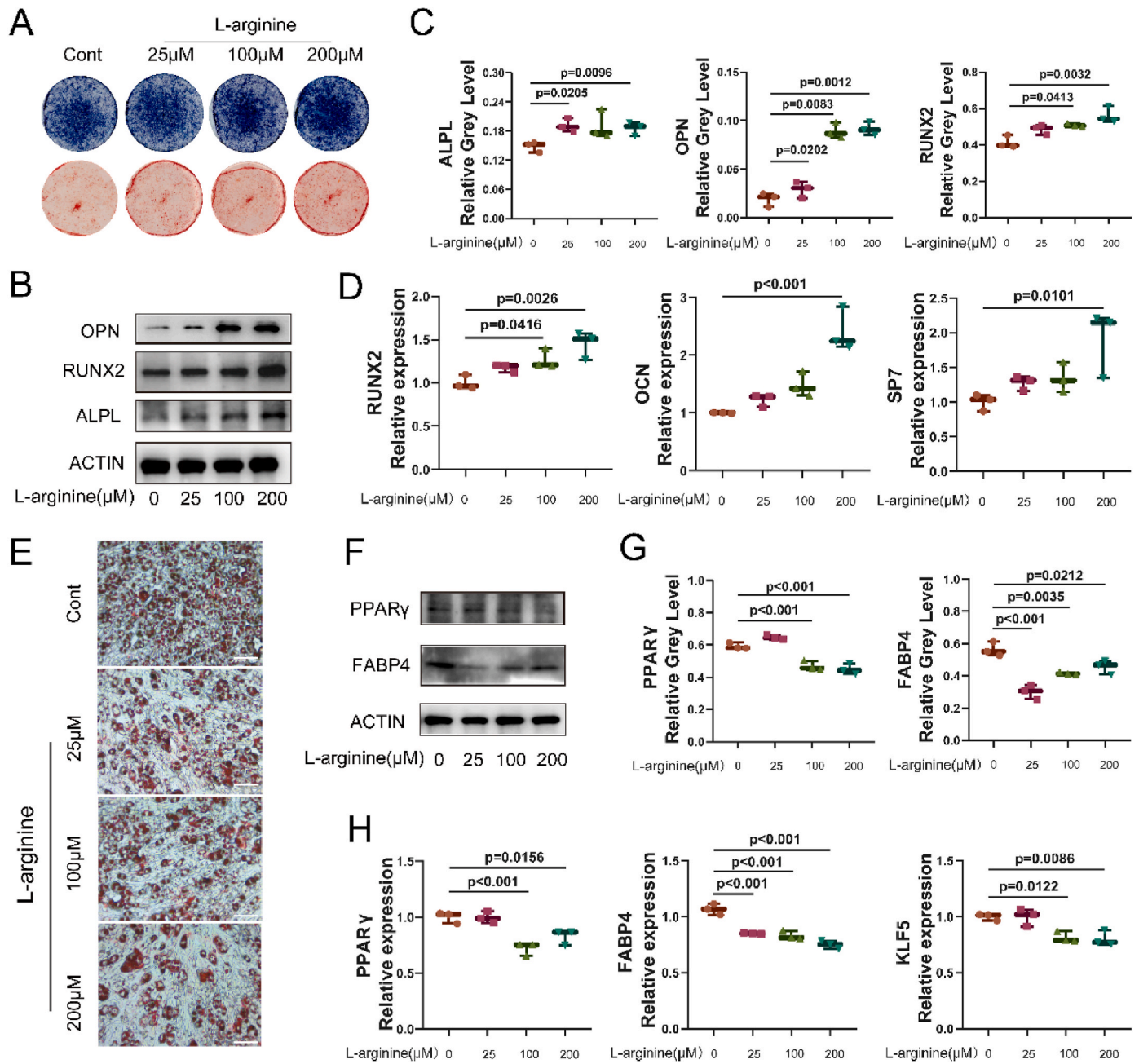


Figure 2. L-arginine promotes angio-osteogenesis but inhibits lipogenesis in vitro. (A) ALP and ARS staining of osteoblasts by different concentrations of L-arginine (n = 3). (B) Western blot of osteoblasts by different concentrations of L-arginine. (C) Quantification of the ratio of band intensity of ALPL, OPN and RUNX2 relative to ACTIN of osteoblasts (n = 3). (D) mRNA expression of *Runx2*, *Ocn* and *Sp7* relative to *Actin* of osteoblasts (n = 3). (E) Oil red O staining of C3H10 cells by different concentrations of L-arginine. Scale bar = 200 μm (n = 3). (F) Western blot of C3H10 cells by different concentrations of L-arginine. (G) Quantification of the ratio of band intensity of PPARγ and FABP4 relative to ACTIN of C3H10 cells (n = 3). (H) mRNA expression of *Pparγ*, *Fabp4* and *Klf5* relative to *Actin* of C3H10 cells (n = 3). (For interpretation of the references to color in this figure legend, the reader is referred to the Web version of this article.)

incubation in 5% bovine serum albumin buffer, the samples were incubated with primary antibodies overnight and then incubated with the secondary antibody for 60 min, washed with phosphate-buffered saline (PBS), and stained with 4',6-diamidino-2-phenylindole (DAPI; Beyotime). For mitochondrial staining, osteoblasts, HUVECs, or C3H10 cells were transfected with LC3 adenovirus, treated with MitoTracker (Beyotime), and fixed with 4% paraformaldehyde.

2.11. Mouse model and calcein dual fluorescent labeling

Animal experiments were performed according to the NIH Guide for the Care and Use of Laboratory Animals. Ten C57BL/6 mice (female

mice, 12 months old) were randomly assigned to the vehicle and L-arginine groups. Mice in the L-arginine group were given water containing dissolved L-arginine for two months and euthanized [22]. For the ovariectomized (OVX) mouse model, 20C57BL/6 mice (female, 12 weeks old) were randomly assigned to four groups (sham, vehicle, parathyroid hormone (PTH), and L-arginine), five mice per group. The sham group was subjected to a sham operation, whereas the vehicle, PTH, and L-arginine groups were subjected to ovariectomy. After four weeks, mice were i.p. injected with PBS (sham and vehicle group), 10 μg/kg PTH (PTH group), or 80 mg/kg L-arginine (L-arginine group) twice per week for six weeks. All mice were i.p. injected with calcein at 10 and 3 d before being euthanized. Femurs were separated and fixed in 4%

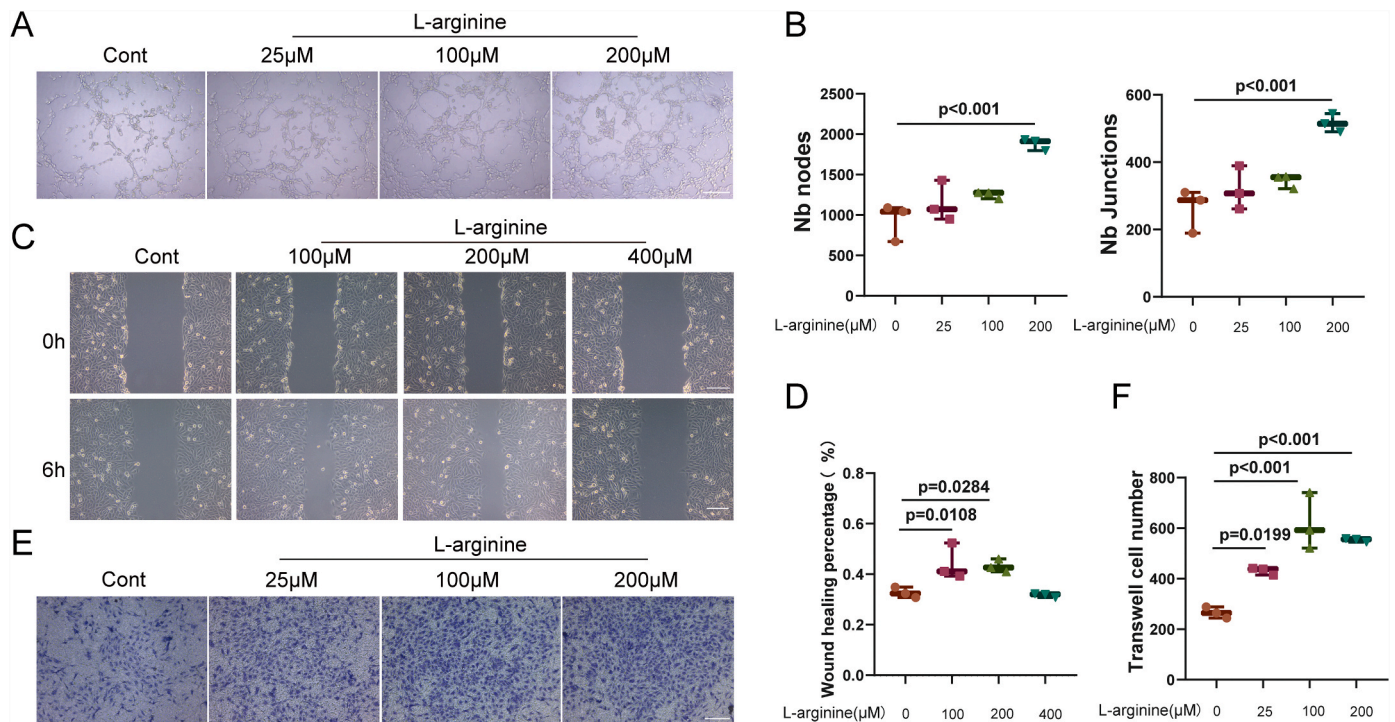


Figure 3. L-arginine promotes angiogenesis in a concentration-dependent manner in vitro. (A) Tube-forming results of HUVECs by different concentrations of L-arginine. Scale bar = 200 μm. (B) Quantitative analyses of Nb.nodes and Nb.junctions of tube forming results (n = 3). (C) Wound healing experiments of HUVECs for 6h by different concentrations of L-arginine. Scale bar = 200 μm. (D) Quantitative analyses of wound healing percentage of wound healing results (n = 3). (E) Transwell results of HUVECs by different concentrations of L-arginine. Scale bar = 200 μm. (F) Quantitative analyses of transwell cell number of transwell results (n = 3).

paraformaldehyde for immunofluorescence and micro-computed tomography (μCT).

2.12. μCT scanning

Mouse femurs were scanned with a Micro CT instrument (Skyscan, Antwerp, Belgium). Trabecular bone volume per total volume (BV/TV), mean trabecular separation (Tb.Sp), mean trabecular number (Tb.N), mean trabecular thickness (Tb.Th), and bone mineral density (BMD) were measured as previously reported [23].

2.13. Statistical analysis

The data was analyzed by GraphPad Prism (GraphPad Software, Boston, USA). Statistical differences were determined using a one-way ANOVA followed by Tukey's post hoc analysis or Student's t test. Differences were considered significant at $p < 0.05$ (two-tailed test).

3. Results

3.1. L-arginine promotes bone formation in mildly aged mice

Firstly, we investigated whether L-arginine could affect bone mass changes when fed to 12-month-old elder female mice. After two months of L-arginine supplementation, μCT demonstrated more bone mass in the L-arginine group than in the vehicle group (Fig. 1A). Quantitative analysis revealed that the BV/TV, Tb.Th, Tb.N, cortical thickness (Cor.Th), and BMD were significantly increased, whereas Tb.Sp was markedly decreased in the L-arginine group (Fig. 1B). Masson's trichrome staining indicated more active osteoblasts in the L-arginine group than in the vehicle group (Fig. 1C). Hematoxylin and eosin (H&E), von Kossa, and osteocalcin (OCN) staining also demonstrated the enhancement of bone formation in the L-arginine group (Fig. 1D and E). Notably, we observed

significantly lower perilipin expression in the L-arginine group than in the vehicle group (Fig. 1D and E), which suggested that L-arginine led to less adipogenesis. Calcein dual fluorescent labeling demonstrated that L-arginine increased the mineral apposition rate (MAR) and bone formation rate per unit of the bone surface of the femur (Fig. 1F and G). Considering the close association between osteogenesis and angiogenesis, we performed immunofluorescence staining for the vascular marker CD31/EMCN, which indicated that L-arginine significantly promoted angiogenesis in vivo (Fig. 1H). Collectively, these results suggest that L-arginine promotes bone formation in elder mice by promoting osteogenesis and angiogenesis and inhibiting adipogenesis.

3.2. L-arginine promotes osteogenesis but inhibits adipogenesis in vitro

To further investigate the effect of L-arginine on osteogenesis, we treated osteoblasts with different concentrations of L-arginine. These concentrations had no effect on cell activity (Supplementary Figs. 1A and B). The ALP and ARS assays revealed that L-arginine promoted osteogenesis in a concentration-dependent manner (Fig. 2A; Supplementary Fig. 1C). In addition, western blotting results showed that the expression of osteoblast-specific proteins, including osteopontin (OPN), RUNX2, and ALP, increased after L-arginine treatment (Fig. 2B and C). Meanwhile, the expression levels of Runx2, Opn, and Sp7 increased (Fig. 2D). Given the in vivo results, we investigated the effect of L-arginine on adipogenesis in C3H10 cells. Fewer adipocytes were observed after L-arginine treatment (Fig. 2E; Supplementary Fig. 1D). Further, the protein expression of PPAR-γ and FABP4 was decreased (Fig. 2F and G), as was the mRNA expression of Ppar-γ, Fabp4, and Klf5 (Fig. 2H). However, we did not observe significant effects of L-arginine on osteoclasts (Supplementary Fig. 1E). In conclusion, our data demonstrate that L-arginine promotes osteogenesis and inhibits adipogenesis.

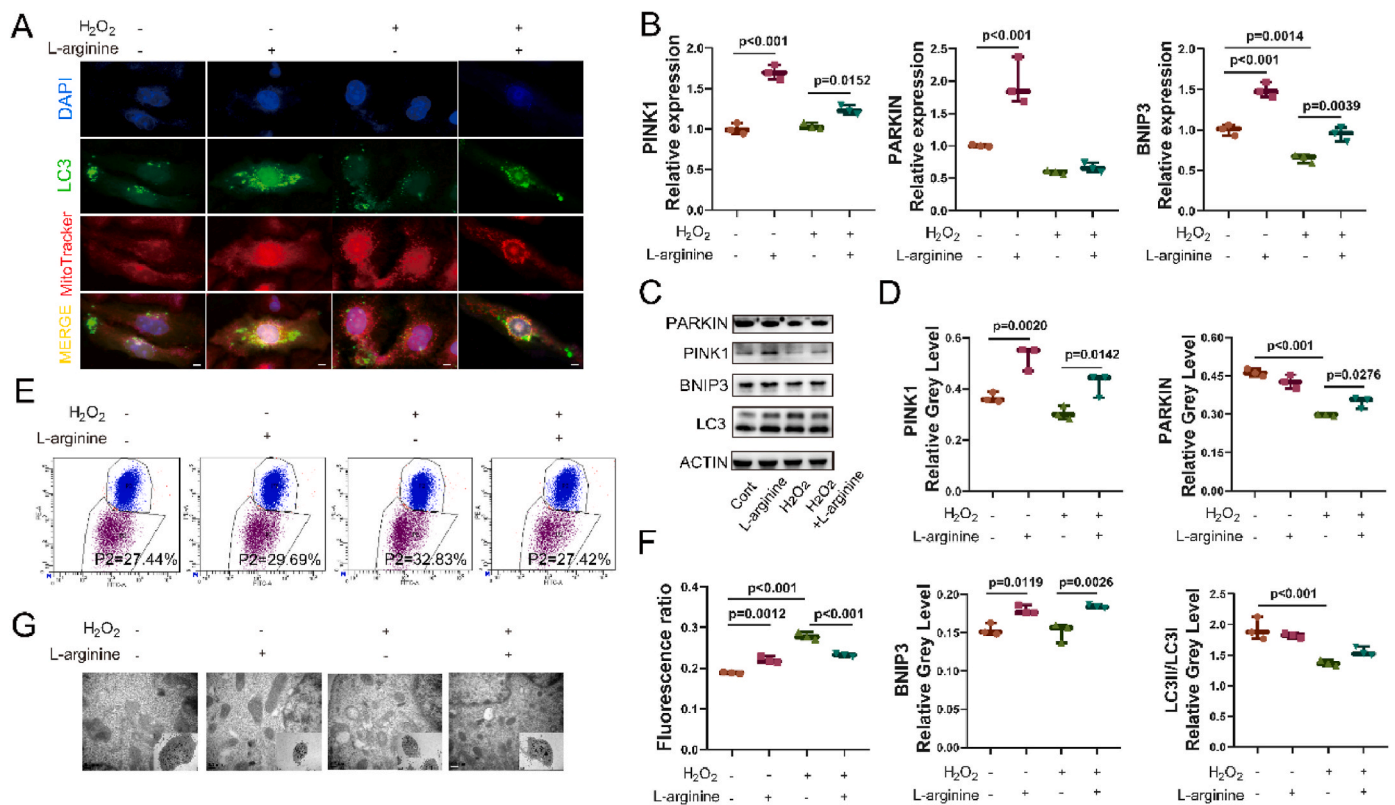


Figure 4. L-arginine rescues endothelial cells from ROS by affecting mitophagy. (A) Immunofluorescence of Mitotracker (red)-LC3 (green)-DAPI (blue) of HUVECs. Cells were treated with H₂O₂ (200 μM) or L-arginine (200 μM) for 24h. Scale bar = 10 μm. (B) mRNA expression of *Pink1*, *Parkin* and *BNIP3* relative to *Actin* of HUVECs (n = 3). (C) Western blot of HUVECs. (D) Quantification of the ratio of band intensity of PINK1, PARKIN, BNIP3 and LC3 relative to ACTIN of HUVECs (n = 3). (E) Flow cytometry of HUVECs with JC-1. HUVECs were treated with H₂O₂ or L-arginine for 24h. (F) Quantitative analyses of fluorescence ratio of flow cytometry results. (G) Transmission electron microscope of HUVECs treated by H₂O₂ or L-arginine for 24h. Scale bar = 0.2 μm (n = 3). (For interpretation of the references to color in this figure legend, the reader is referred to the Web version of this article.)

3.3. L-arginine promotes angiogenesis in a concentration-dependent manner in vitro

We investigated the role of L-arginine in angiogenesis in vitro using HUVECs. After determining the appropriate concentration of L-arginine (Supplementary Fig. 2A), we found that L-arginine promoted the tube-forming ability of HUVECs and increased the number of nodes and junctions (Fig. 3A and B). Specifically, wound healing (Fig. 3C and D) and cell migration experiments (Fig. 3E and F) demonstrated positive results after treatment with L-arginine. Notably, the promoting effect of L-arginine on these parameters was the most significant at a concentration of 200 μM. BEC-HCl is a competitive arginase II inhibitor [24]. Interestingly, BEC-HCl treatment decreased the tube-forming ability of HUVECs (Supplementary Figs. 2B–D) and cell migration (Supplementary Figs. 2E and F). Collectively, L-arginine promotes angiogenesis in HUVECs in vitro, whereas BEC-HCl inhibits this process.

3.4. L-arginine rescues endothelial and osteoblast-lineage cells from ROS by affecting mitophagy

We further investigated whether L-arginine could promote angiogenesis by affecting mitochondria. We treated HUVECs with H₂O₂ to induce the production of ROS, which can interact with cellular proteins, nucleic acids, and lipids to induce oxidative stress and disrupt the balance between oxidation- and reduction-regulated cellular processes, ultimately causing oxidative damage. After H₂O₂ treatment, abnormal mitochondrial morphology was observed. Mitochondria displayed an increase in fragment structure staining based on MitoTracker, and co-localization with LC3 staining showed that L-arginine promoted

mitophagy (Fig. 4A). We also investigated the expression of mitophagic genes, including *Pink1*, *Parkin*, and *BNIP3*. Their mRNA expressions of these genes were increased after L-arginine treatment, with and without H₂O₂ treatment (Fig. 4B). The protein expression of PINK1 and *Parkin* showed the same trend, whereas an increase in BNIP3 was observed in L-arginine-treated cells exposed to H₂O₂-induced ROS (Fig. 4C and D). Additionally, H₂O₂ promoted the accumulation of JC-1 monomers in mitochondria, indicating low membrane potential, whereas L-arginine rescued this phenotype (Fig. 4E and F). To further validate its effects on mitochondria, we treated HUVECs with L-arginine and examined them using transmission electron microscopy (TEM). After H₂O₂ treatment, mitochondria were severely damaged and appeared to be vacuolated, which was reversed by L-arginine treatment (Fig. 4G). Notably, BEC-HCl treatment downregulated the expression of PINK1, *Parkin*, and BNIP3 (Supplementary Figs. 3A and B). We also observed a decrease in the membrane potential of mitochondria (Supplementary Figs. 3C and D). Interestingly, the TEM images demonstrated vacuolated mitochondria after BEC-HCl treatment (Supplementary Fig. 3E). These results prove that L-arginine promotes angiogenesis and rescues cells from the effects of H₂O₂-induced ROS by affecting mitochondria and possibly changing the level of mitophagy.

Next, we investigated whether L-arginine could still influence osteoblasts or adipocytes when they were challenged by oxidative stress. The ALP and ARS assays revealed that H₂O₂ decreased the activity of osteoblasts, whereas L-arginine reversed this effect (Fig. 5A and B). L-arginine also reversed the reduction in mitochondrial membrane potential caused by H₂O₂ (Fig. 5C and D). In addition, we observed damaged mitochondria in H₂O₂-treated osteoblasts using LC3-MitoTracker mitochondrial co-localization staining (Fig. 5E). We found that the co-

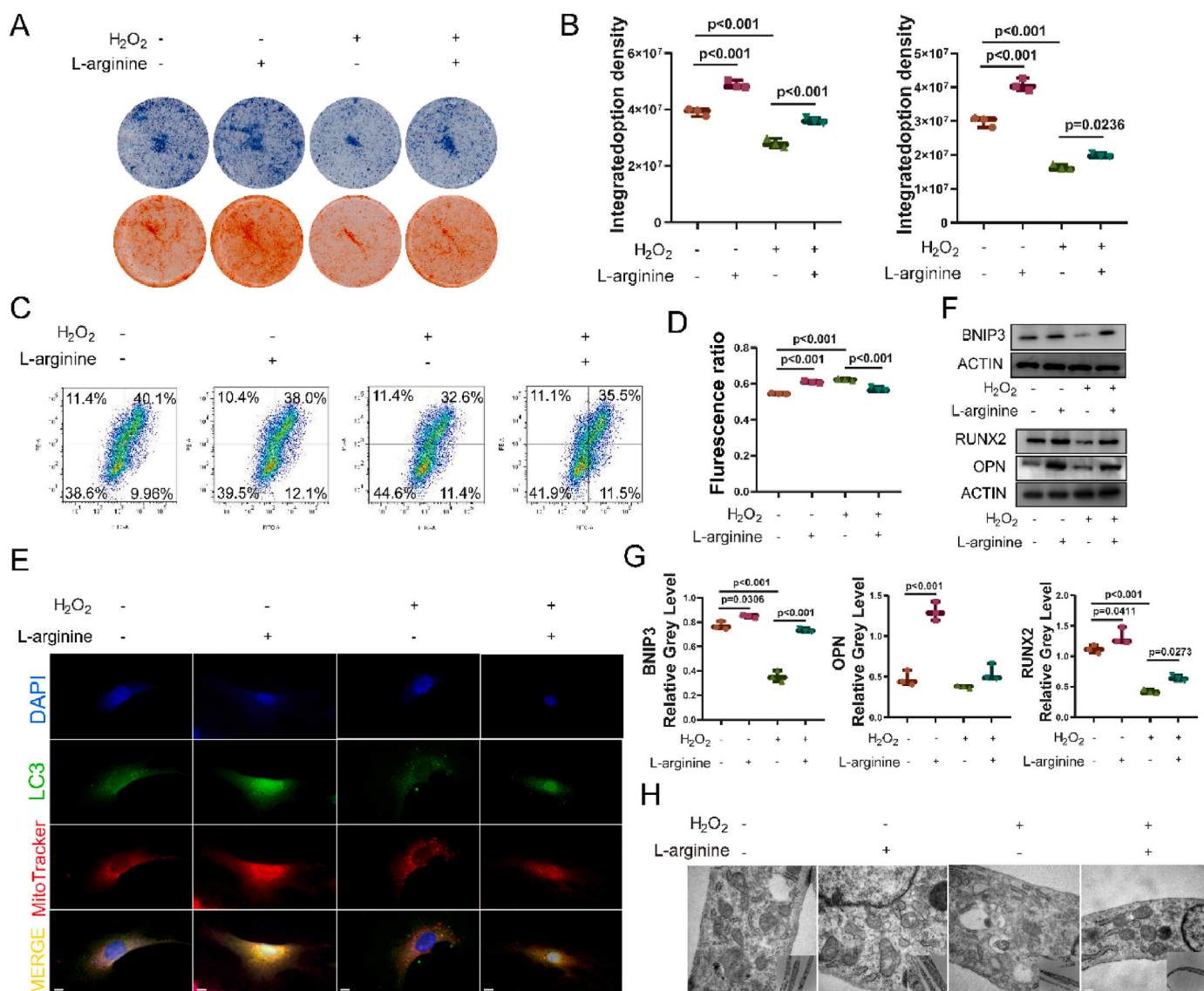


Figure 5. L-arginine rescues osteoblasts from ROS by affecting mitophagy. (A) ALP and ARS staining of osteoblasts treated by H₂O₂ (200 μM) or L-arginine (200 μM) for 24h. (B) Quantitative analyses of integrated optical density of ALP(left) and ARS(right) (n = 3). (C) Flow cytometry of osteoblasts with JC-1. Osteoblasts were treated with H₂O₂ or L-arginine for 24h. (D)Quantitative analyses of fluorescence ratio of flow cytometry results. (E)Immunofluorescence of Mitotracker(red)-LC3 (green)-DAPI(blue) of osteoblasts. Cells were treated with H₂O₂ (200 μM) or L-arginine (200 μM) for 24h. Scale bar = 10 μm. (F) Western blot of osteoblasts treated with H₂O₂ or L-arginine for 24h(up) or 1week(down). BNIP3 protein was detected in early stage, RUNX2 and OPN proteins were detected in late stage. (G) Quantification of the ratio of band intensity of BNIP3, OPN and RUNX2 relative to ACTIN of osteoblasts(n = 3). (H) Transmission electron microscope of osteoblasts treated by H₂O₂ or L-arginine for 24h. Scale bar = 0.2 μm(n = 3). (For interpretation of the references to color in this figure legend, the reader is referred to the Web version of this article.)

localization of Mitotracker and LC3 was reduced after BEC-HCl treatment (Supplementary Fig. 4A). Western blotting results also showed that L-arginine could rescue the decrease in BNIP3 protein expression induced by H₂O₂ at an early stage, whereas the expression of osteogenesis-related proteins, such as RUNX2 and OPN, was rescued at a later stage (Fig. 5F and G). TEM confirmed the results of the mitochondrial staining (Fig. 5H). Next, we performed the same experiments using adipocytes. L-arginine reduced adipocyte formation following H₂O₂ treatment (Fig. 6A). Moreover, flow cytometric analysis after JC-1 treatment demonstrated that L-arginine could effectively prevent the decrease in mitochondrial membrane potential caused by H₂O₂ treatment (Fig. 6B and C). LC3-Mitotracker mitochondrial co-localization staining indicated low membrane potential and rescue of this phenotype by L-arginine (Fig. 6D). Conversely, decreased co-localization was observed in C3H10 cells after BEC-HCl treatment (Supplementary Fig. 4B). In addition, we observed the upregulation of Bnip3 expression

after L-arginine treatment. The upregulation of FABP4 expression was observed in C3H10 cells after H₂O₂ treatment, whereas FABP4 expression was significantly reduced by the simultaneous addition of L-arginine. However, no significant alteration was observed in CEBPα or PPARγ levels (Fig. 6E and F). Similar results to those for osteoblasts were obtained with C3H10 cells, as revealed by TEM assay (Fig. 6G). These results show that L-arginine protects cells from H₂O₂-induced ROS by affecting the mitochondria and possibly changing the level of mitophagy.

3.5. L-arginine promotes bone formation in OVX mice by promoting angiosteo genesis

Based on our findings, we were interested in whether L-arginine could exert a protective effect against ovariectomy-induced osteoporosis in mice. Compared to the sham group, the vehicle group showed

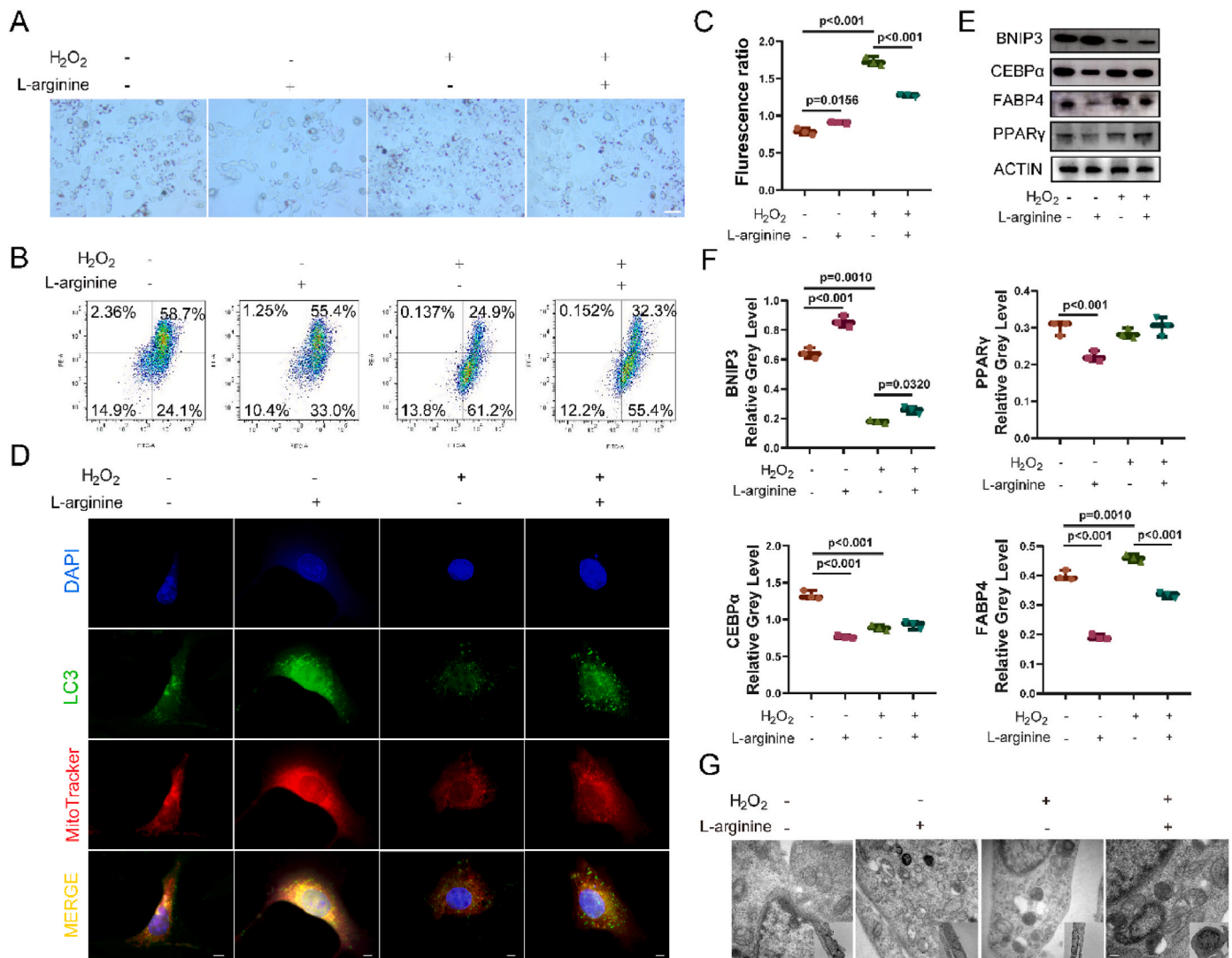


Figure 6. L-arginine rescues C3H10 cells from ROS by affecting mitophagy. (A) Oil red O staining of C3H10 cells treated with H₂O₂ or L-arginine for 24h. Scale bar = 200 μm. (B) Flow cytometry of C3H10 cells with JC-1. C3H10 cells were treated with H₂O₂ (200 μM) or L-arginine (200 μM) for 24h. (C) Quantitative analyses of fluorescence ratio of flow cytometry results. (D) Immunofluorescence of Mitotracker(red)-LC3(green)-DAPI(blue) of C3H10 cells. Cells were treated with H₂O₂ or L-arginine for 24h. Scale bar = 10 μm. (E) Western blot of C3H10 cells treated with H₂O₂ (200 μM) or L-arginine (200 μM) for 24h. BNIP3, and adipogenic associated proteins CEBPα, FABP4, PPARγ were detected. (F) Quantification of the ratio of band intensity of BNIP3, CEBPα, FABP4 and PPARγ relative to ACTIN of osteoblasts(n = 3). (G) Transmission electron microscope of C3H10 cells treated by H₂O₂ or L-arginine for 24h. Scale bar = 0.2 μm(n = 3). (For interpretation of the references to color in this figure legend, the reader is referred to the Web version of this article.)

significant bone loss based on μCT, which was prevented by PTH or L-arginine treatment (Fig. 7A). Quantitative analysis revealed that BT/TV, Tb.N, Tb.Th, and Cor.Th were significantly decreased, and Tp.Sp was increased in the OVX-vehicle group, whereas these changes were reversed by PTH or L-arginine, except for Tb.Sp (Fig. 7B and C). Dual fluorescent labeling with calcein demonstrated that L-arginine could increase the MAR of the femur in OVX mice (Fig. 7D and E). Moreover, H&E staining demonstrated a decrease in trabecular bone in the vehicle group, whereas PTH or L-arginine treatment improved this. This result was confirmed through von Kossa and Masson’s trichrome staining of femurs (Fig. 7F). Meanwhile, expression of the osteogenesis-related gene OCN was decreased in the vehicle group compared with that in the sham group, whereas L-arginine or PTH reversed this effect (Fig. 8A and B). In addition, the upregulation of perilipin expression in the vehicle group was suppressed in the L-arginine and PTH groups (Fig. 8C and D). In situ staining for CD31/EMCN demonstrated a decrease in vessel formation in the vehicle group, which was improved by L-arginine or PTH (Fig. 8E). Taken together, L-arginine attenuates OVX-induced osteoporosis,

suggesting a possible therapeutic potential.

4. Discussion

Osteoporosis is a serious disease that affects middle-aged and elderly individuals worldwide, especially postmenopausal women. With aging, bone homeostasis becomes disordered, the activity of osteoblasts decreases, osteoclasts become abnormally active, osteoporosis occurs, and the risk of fracture increases significantly. Currently, most drugs used for osteoporosis treatment, such as denosumab and bisphosphonates, target osteoclasts, inhibiting their activity and reducing bone resorption, thereby delaying the progression of osteoporosis [5]. In this study, we found that the semi-essential amino acid L-arginine could promote osteogenesis while acting on other cells in the bone microenvironment to counteract the effect of oxidative stress on bone homeostasis. Additionally, we found that this process might occur through mitophagy mediated by the Bnip3 or PINK1/Parkin pathways, indicating that mitophagy plays a key role in the maintenance of bone homeostasis.

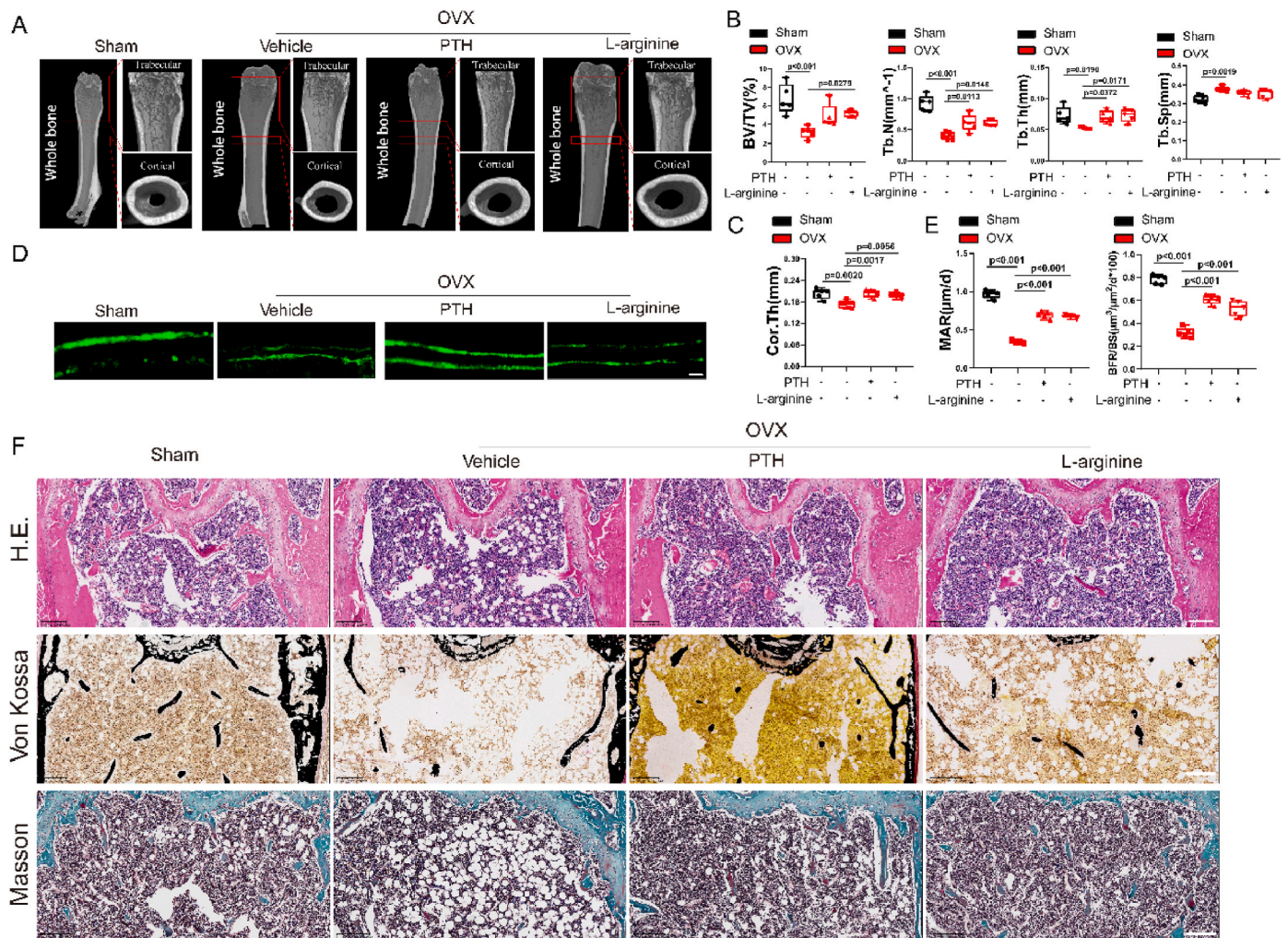


Figure 7. L-arginine promotes bone formation in OVX mice by promoting angio-osteogenesis. (A) Representative micro-CT images of proximal femurs from sham group, vehicle group, PTH group and L-arginine group. (B) Quantitative analyses of BV/TV, Tb.N, Tb,Sp and Tb.Th (n = 5 per group). (C) Quantitative analyses of Cor.Th (n = 5 per group). (D) Representative images of Calcein double fluorescent labeling in mouse femurs of 4 groups. Scale bar = 5 µm. (E) Quantitative analyses of MAR and BFR/BS (n = 5 per group). (F) Representative images of H.E., Von Kossa and Masson staining of femurs from 4 groups. Scale bar = 300 µm (Masson) or 200 µm (H.E. and Von Kossa).

Angiogenesis and bone formation are inextricably linked. Within bone tissue, angiogenesis is regulated by signaling factors secreted by various cells in bones and blood vessels, which influence the formation of new bones [25]. Furthermore, changes in the skeletal microvasculature can influence abnormal bone formation in patients with osteoporosis [26]. Previous studies have shown that during fracture repair, osteoblasts secrete vascular endothelial growth factor A that promotes macrophage recruitment and angiogenesis, initiating the repair process [27]. Osteogenic precursor cells also co-invade vascular endothelial cells during fractured cartilage repair and promote healing [28]. Type H vessels were recently found to be located near the metaphyseal growth plate, which exhibits a high expression of endomucin and CD31. Type H vessels produce specific factors, stimulate the proliferation and differentiation of bone marrow cells, and promote bone formation. Mildly aged or OVX mice demonstrated a decrease in type H vessels, and this decrease was also observed in humans with aging [25,29–31]. In addition, the increased adipogenesis of bone mesenchymal stem cells is another important cause of osteoporosis. With increasing age and changes in hormone secretion after menopause, bone marrow stromal cells (BMSCs) are more inclined toward adipogenic differentiation, and the risk of osteoporosis increases [32,33]. This process is regulated in a variety of ways. The leptin receptor is a nutrient/fat receptor that acts on bone marrow mesenchymal cells to inhibit osteogenesis and promote

adipogenesis. Osteocytes inhibit osteogenesis and promote adipogenesis by secreting neuropeptide Y. IL-11 also controls osteogenesis and systemic obesity under conditions of mechanical loading in the bone [33–35]. It's indicated that the mutual balance between osteogenesis and adipogenesis is a key indicator of bone homeostasis. In this study, we demonstrated that L-arginine significantly improved bone mass in aged and OVX mice, promoting the formation of type H vessels and reducing the production of adipocytes in bones. These results suggest that L-arginine has a positive effect on osteogenesis.

Mitophagy comprises an important regulatory mechanism for the intracellular removal of damaged mitochondria, ensuring an effective population of functional mitochondria. In the classical mitophagic pathway, damaged mitochondria cause the accumulation of PINK1 and Parkin, promoting the separation of autophagic degradation. Previous studies have shown that mitophagy works in the progression of neurodegenerative diseases [7,36,37]. In recent years, mitophagy in bone tissues has emerged as an important research topic. Mitophagy is involved in the regulation of osteoporosis, degenerative arthritis, and other bone diseases. The attenuation of mitophagy under oxidative stress can accumulate ROS in damaged mitochondria, which further promotes the differentiation and maturation of osteoclasts mediated by inflammatory factors [38–41]. During the osteogenic differentiation of osteoblasts, mitochondrial biogenesis, function, and ATP content

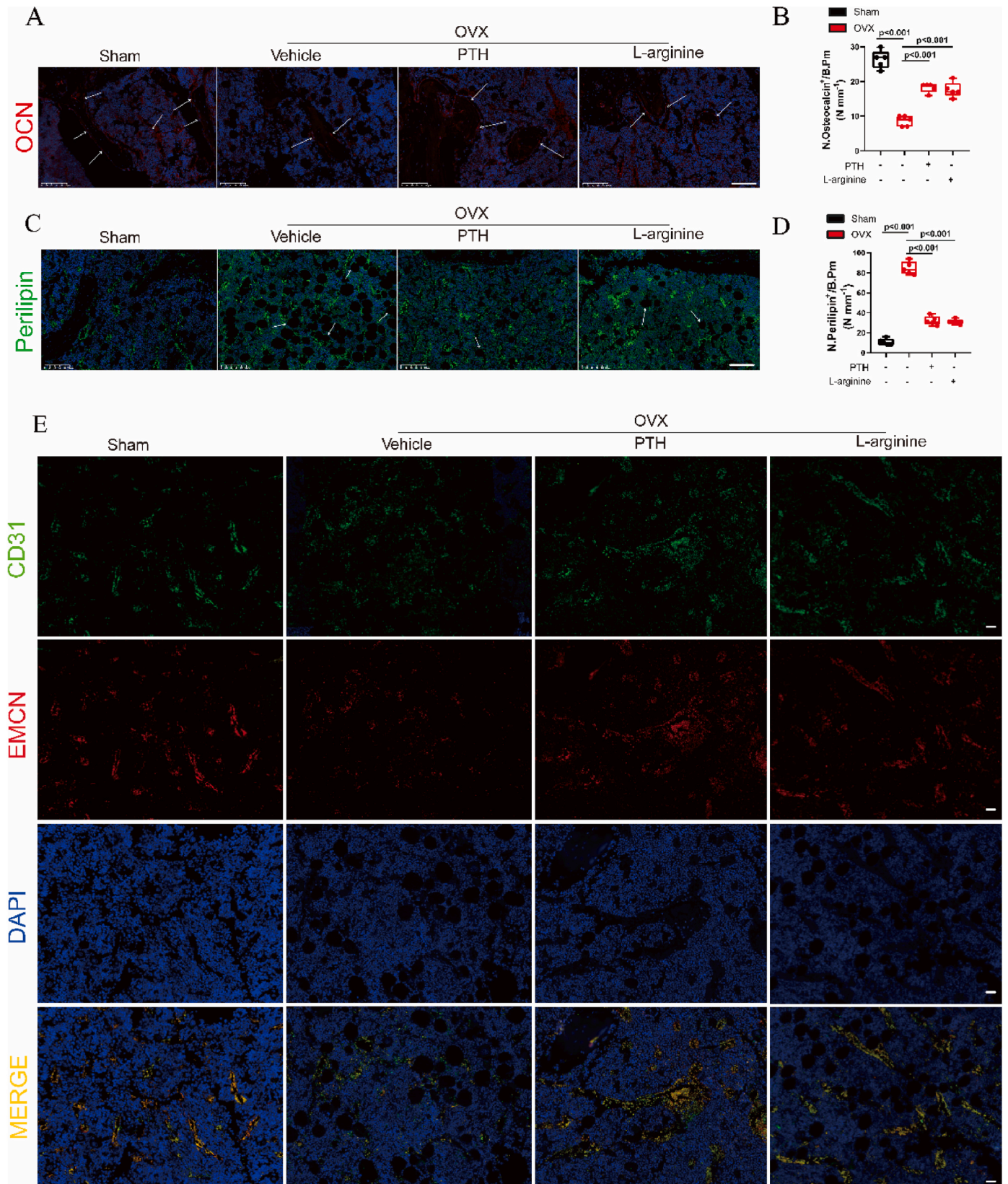


Figure 8. L-arginine promotes bone formation in OVX mice by promoting angio-osteogenesis. (A) Representative immunofluorescence images of OCN staining of decalcified bone sections from 4 groups. Scale bar = 200 μ m. (B) Quantitative analyses of Mean gray value of OCN Immunostaining (n = 3 per group). (C) Representative immunofluorescence images of perilipin staining of decalcified bone sections from 4 groups. Scale bar = 200 μ m. (D) Quantitative analyses of OCN and Perilipin positive cells in femora (n = 5 per group). (E) Immunostaining of CD31 (green) and EMCN (red) in femora from 4 groups. Scale bar = 20 μ m. (For interpretation of the references to color in this figure legend, the reader is referred to the Web version of this article.)

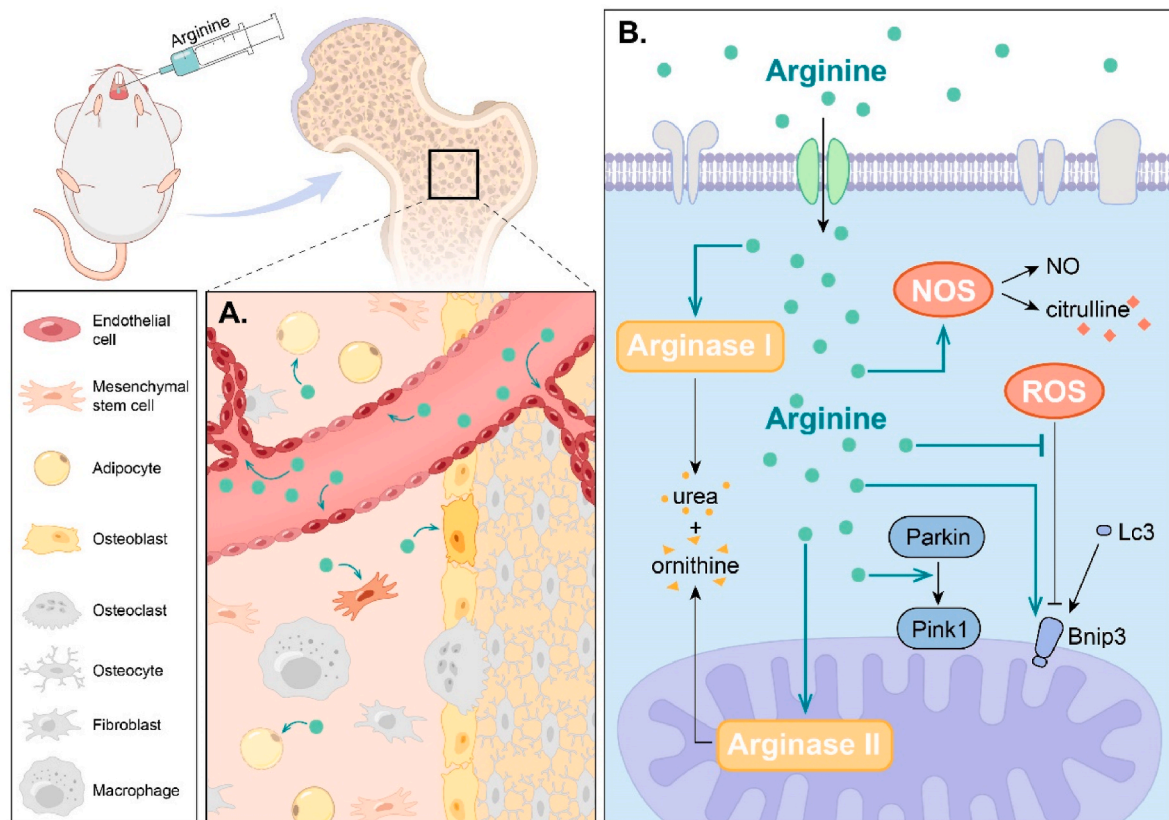


Figure 9. A schematic of proposed mechanism of L-arginine maintaining bone homeostasis. (A) There are many types of cells in bone tissue. The addition of L-arginine can trigger the activity of endothelial cells, osteoblasts, mesenchymal stem cells, etc., promote osteogenic differentiation, inhibit adipogenic differentiation and promote angiogenesis. **(B)** After entering cells, L-arginine promotes the expression of mitochondrial proteins PINK1, PARKIN and BNIP3, and promotes the occurrence of mitophagy. Meanwhile, L-arginine could inhibit the decrease of Bnip3 expression in ROS state, and initiate mitophagy clearance of damaged mitochondria to protect cells. Notably, there are two pathways of L-arginine decomposition in the cells, by NOS and by arginase. The pathway of arginase II decomposition in mitochondria might be involved in the regulation of L-arginine on mitophagy. (For interpretation of the references to color in this figure legend, the reader is referred to the Web version of this article.)

significantly increase. Damaged mitochondria release ROS and apoptotic factors, leading to the death or apoptosis of osteoblasts; however, damaged mitochondria are also degraded through mitophagy, thereby protecting osteoblasts [39,42]. Interestingly, increased ROS levels and mitochondrial dysfunction were also observed during BMSC senescence, whereas increased autophagy could delay the process [43–45]. In this study, we demonstrated the positive effects of L-arginine on mitophagy in multiple cell types. By promoting the expression of Bnip3, L-arginine can protect cells against ROS. Recent studies have proven that the Bnip3 pathway regulates mitophagy during hypoxia [46]. These results suggest that mitophagy plays a pivotal role in bone homeostasis in osteoblasts, osteoclasts, and BMSCs. Notably, we found that the regulation of mitophagy-related proteins by L-arginine was inhibited by arginase II. The occurrence of osteoporosis is associated with an elevated level of oxidative stress, but the catabolism of L-arginine via the NO pathway is inhibited under oxidative stress [47,48]. This finding suggested that the effect of L-arginine on mitophagy might be specifically related to its metabolic pathway in the cell and implied that arginase II might participate in regulating L-arginine-mediated mitophagy. We will further explore this possibility in subsequent studies.

In conclusion, L-arginine was found to delay osteoporosis in mildly aged mice. In vitro experiments demonstrated that L-arginine could promote PINK1/Parkin- and Bnip3-mediated mitophagy, promote osteogenesis and angiogenesis, and inhibit adipogenesis. Furthermore, L-arginine may protect against bone formation in the presence of ROS. It was demonstrated that L-arginine can play a role in the maintenance of bone homeostasis (Fig. 9). The efficacy of L-arginine in preventing

osteoporosis was further demonstrated in an OVX mouse model. Therefore, our work provides more insight into the relationship between L-arginine, mitophagy, and bone remodeling and suggests that L-arginine has the potential to be used as an adjuvant nutrient for the treatment of osteoporosis.

Funding statement

This work was supported by the National Natural Science Foundation of China (grant number 82102591, 82372440, 81972089, 82002334, 82101647); The Key Project of National Natural Science Foundation of China (grant number 82330077); Natural Science Foundation of Zhejiang Province (grant number LQ22H060001, Y23H060039, Z20H060003, Q20H060042); Zhejiang Medical and Health Science and Technology Program (grant number 2016KYB326); Union Fund Project of National Natural Science Foundation of China (grant number U21A20351).

CRediT authorship contribution statement

Yang Shen: Methodology, Validation, Formal analysis, Investigation, Data curation, Writing – original draft. **Haoming Wang:** Validation, Formal analysis, Data curation. **Hongwei Xie:** Investigation, Writing – review & editing. **Jiateng Zhang:** Writing – review & editing. **Qingliang Ma:** Methodology. **Shiyu Wang:** Methodology, Writing – review & editing. **Putao Yuan:** Formal analysis, Resources. **Hong Xue:** Formal analysis. **Huaxing Hong:** Funding acquisition. **Shunwu Fan:**

Funding acquisition. **Wenbin Xu:** Funding acquisition. **Ziang Xie:** Supervision, Funding acquisition, Writing – review & editing.

Declaration of competing interest

All authors state that they have no conflicts of interest.

Acknowledgements

The institutional review board and ethics committee of Sir Run Run Shaw Hospital, Zhejiang University School of Medicine, examined and approved the study.

Appendix A. Supplementary data

Supplementary data to this article can be found online at <https://doi.org/10.1016/j.jot.2024.03.003>.

References

- Rodan GA, Martin TJ. Therapeutic approaches to bone diseases. *Science* 2000;289(5484):1508–14.
- Greenwood C, Clement J, Dicken A, Evans P, Lyburn I, Martin RM, et al. Age-related changes in femoral head trabecular microarchitecture. *Aging Dis* 2018;9(6):976–87.
- Ensrud KE, Crandall CJ. Osteoporosis. *Ann Intern Med* 2017;167(3):ITC17–32.
- Compston JE, McClung MR, Leslie WD. Osteoporosis. *Lancet* 2019;393(10169):364–76.
- Reid IR, Billington EO. Drug therapy for osteoporosis in older adults. *Lancet* 2022;399(10329):1080–92.
- Khosla S, Hofbauer LC. Osteoporosis treatment: recent developments and ongoing challenges. *Lancet Diabetes Endocrinol* 2017;5(11):898–907.
- Mizushima N, Levine B. Autophagy in human diseases. *N Engl J Med* 2020;383(16):1564–76.
- Levine B, Kroemer G. Biological functions of autophagy genes: a disease perspective. *Cell* 2019;176(1–2):11–42.
- Guo YF, Su T, Yang M, Li CJ, Guo Q, Xiao Y, et al. The role of autophagy in bone homeostasis. *J Cell Physiol* 2021;236(6):4152–73.
- Bravo-San Pedro JM, Kroemer G, Galluzzi L. Autophagy and mitophagy in cardiovascular disease. *Circ Res* 2017;120(11):1812–24.
- Youle RJ, Narendra DP. Mechanisms of mitophagy. *Nat Rev Mol Cell Biol* 2011;12(1):9–14.
- Kerr JS, Adriaanse BA, Greig NH, Mattson MP, Cader MZ, Bohr VA, et al. Mitophagy and Alzheimer's disease: cellular and molecular mechanisms. *Trends Neurosci* 2017;40(3):151–66.
- Jin Q, Li R, Hu N, Xin T, Zhu P, Hu S, et al. DUSP1 alleviates cardiac ischemia/reperfusion injury by suppressing the Mif-required mitochondrial fission and Bnip3-related mitophagy via the JNK pathways. *Redox Biol* 2018;14:576–87.
- Li Q, Qi F, Meng X, Zhu C, Gao Y. Mst1 regulates colorectal cancer stress response via inhibiting Bnip3-related mitophagy by activation of JNK/p53 pathway. *Cell Biol Toxicol* 2018;34(4):263–77.
- Zhang J, Ney PA. Role of BNIP3 and NIX in cell death, autophagy, and mitophagy. *Cell Death Differ* 2009;16(7):939–46.
- Alvares TS, Conte CA, Paschoalin VM, Silva JT, Meirelles CdeM, Bhamhani YN, et al. Acute l- supplementation increases muscle blood volume but not strength performance. *Appl Physiol Nutr Metabol* 2012;37(1):115–26.
- Gogoi M, Datey A, Wilson KT, Chakravorty D. Dual role of metabolism in establishing pathogenesis. *Curr Opin Microbiol* 2016;29:43–8.
- Mocchegiani E, Santarelli L, Costarelli L, Cipriano C, Muti E, Giacconi R, et al. Plasticity of neuroendocrine-thymus interactions during ontogeny and ageing: role of zinc and. *Ageing Res Rev* 2006;5(3):281–309.
- Xie Z, Hou L, Shen S, Wu Y, Wang J, Jie Z, et al. Mechanical force promotes dimethyl dimethylaminohydrolyase 1-mediated hydrolysis of the metabolite asymmetric dimethyl to enhance bone formation. *Nat Commun* 2022;13(1):50.
- Chen S, Jin G, Huang KM, Ma JJ, Wang Q, Ma Y, et al. Lycorine suppresses RANKL-induced osteoclastogenesis in vitro and prevents ovariectomy-induced osteoporosis and titanium particle-induced osteolysis in vivo. *Sci Rep* 2015;5:12853.
- Xie Z, Yu H, Sun X, Tang P, Jie Z, Chen S, et al. A novel diterpenoid suppresses osteoclastogenesis and promotes osteogenesis by inhibiting Irf1-mediated and Ikb- mediated p65 nuclear translocation. *J Bone Miner Res* 2018;33(4):667–78.
- Wei Z, Oh J, Flavell RA, Crawford JM. LACC1 bridges NOS2 and polyamine metabolism in inflammatory macrophages. *Nature*. 2023 Jun;618(7965):E21]. *Nature* 2022;609(7926):348–53.
- Ma Q, Wang S, Xie Z, Shen Y, Zheng B, Jiang C, et al. The SFRP1 inhibitor WAY-316606 attenuates osteoclastogenesis through dual modulation of canonical Wnt signaling. *J Bone Miner Res* 2022;37(1):152–66.
- Colleluori DM, Ash DE. Classical and slow-binding inhibitors of human type II arginase. *Biochemistry* 2001;40(31):9356–62.
- Kusumbe AP, Ramasamy SK, Adams RH. Coupling of angiogenesis and osteogenesis by a specific vessel subtype in bone. *Nature* 2014;507(7492):323–8.
- Burkhardt R, Kettner G, Böhm W, Schmidmeier M, Schlag R, Frisch B, et al. Changes in trabecular bone, hematopoiesis and bone marrow vessels in aplastic anemia, primary osteoporosis, and old age: a comparative histomorphometric study. *Bone* 1987;8(3):157–64.
- Tuckermann J, Adams RH. The endothelium-bone axis in development, homeostasis and bone and joint disease. *Nat Rev Rheumatol* 2021;17(10):608–20.
- Maes C, Kobayashi T, Selig MK, Torrekens S, Roth SI, Mackem S, et al. Osteoblast precursors, but not mature osteoblasts, move into developing and fractured bones along with invading blood vessels. *Dev Cell* 2010;19(2):329–44.
- Ramasamy SK, Kusumbe AP, Wang L, Adams RH. Endothelial Notch activity promotes angiogenesis and osteogenesis in bone. *Nature* 2014;507(7492):376–80.
- Wang L, Zhou F, Zhang P, Wang H, Qu Z, Jia P, et al. Human type H vessels are a sensitive biomarker of bone mass. *Cell Death Dis* 2017;8(5):e2760.
- Peng Y, Wu S, Li Y, Crane JL. Type H blood vessels in bone modeling and remodeling. *Theranostics* 2020;10(1):426–36.
- Li CJ, Xiao Y, Yang M, Su T, Sun X, Guo Q, et al. Long noncoding RNA Bmncr regulates mesenchymal stem cell fate during skeletal aging. *J Clin Invest* 2018;128(12):5251–66.
- Zhang Y, Chen CY, Liu YW, Rao SS, Tan YJ, Qian YX, et al. Neuronal induction of bone-fat imbalance through osteocyte neuropeptide Y. *Adv Sci* 2021;8(24):e2100808.
- Yue R, Zhou BO, Shimada IS, Zhao Z, Morrison SJ. Leptin receptor promotes adipogenesis and reduces osteogenesis by regulating mesenchymal stromal cells in adult bone marrow. *Cell Stem Cell* 2016;18(6):782–96.
- Dong B, Hiasa M, Higa Y, Ohnishi Y, Endo I, Kondo T, et al. Osteoblast/osteocyte-derived interleukin-11 regulates osteogenesis and systemic adipogenesis. *Nat Commun* 2022;13(1):7194.
- Pickles S, Vigié P, Youle RJ. Mitophagy and quality control mechanisms in mitochondrial maintenance. *Curr Biol* 2018;28(4):R170–85.
- Ashrafi G, Schwarz TL. The pathways of mitophagy for quality control and clearance of mitochondria. *Cell Death Differ* 2013;20(1):31–42.
- Sun K, Jing X, Guo J, Yao X, Guo F. Mitophagy in degenerative joint diseases. *Autophagy* 2021;17(9):2082–92.
- Wang S, Deng S, Ma Y, Jin J, Qi F, Li S, et al. The role of autophagy and mitophagy in bone metabolic disorders. *Int J Biol Sci* 2020;16(14):2675–91.
- Deng R, Zhang HL, Huang JH, Cai RZ, Wang Y, Chen YH, et al. MAPK1/3 kinase-dependent ULK1 degradation attenuates mitophagy and promotes breast cancer bone metastasis. *Autophagy* 2021;17(10):3011–29.
- Sun X, Xie Z, Hu B, Zhang B, Ma Y, Pan X, et al. The Nrf2 activator RTA-408 attenuates osteoclastogenesis by inhibiting STING dependent NF- κ B signaling. *Redox Biol* 2020;28:101309.
- Li L, Wang H, Chen X, Li X, Wang G, Jie Z, et al. Oxidative stress-induced hypermethylation of KLF5 promoter mediated by DNMT3B impairs osteogenesis by diminishing the interaction with β -catenin. *Antioxidants Redox Signal* 2021;35(1):1–20.
- Liu F, Yuan Y, Bai L, Yuan L, Li L, Liu J, et al. LRRc17 controls BMSC senescence via mitophagy and inhibits the therapeutic effect of BMSCs on ovariectomy-induced bone loss. *Redox Biol* 2021;43:101963.
- Li M, Yu Y, Xue K, Li J, Son G, Wang J, et al. Genistein mitigates senescence of bone marrow mesenchymal stem cells via ER α -mediated mitochondrial biogenesis and mitophagy in ovariectomized rats. *Redox Biol* 2023;61:102649.
- Guo Y, Jia X, Cui Y, Song Y, Wang S, Geng Y, et al. Sirt3-mediated mitophagy regulates AGES-induced BMSCs senescence and senile osteoporosis. *Redox Biol* 2021;41:101915.
- Madhu V, Boneski PK, Silagi E, Qiu Y, Kurland I, Guntur AR, et al. Hypoxic regulation of mitochondrial metabolism and mitophagy in nucleus pulposus cells is dependent on HIF-1 α -BNIP3 axis. *J Bone Miner Res* 2020;35(8):1504–24.
- Geng Q, Gao H, Yang R, Guo K, Miao D. Pyrroloquinoline quinone prevents estrogen deficiency-induced osteoporosis by inhibiting oxidative stress and osteocyte senescence. *Int J Biol Sci* 2019;15(1):58–68.
- Ma L, Hu L, Feng X, Wang S. Nitrate and nitrite in health and disease. *Aging Dis* 2018;9(5):938–45.